Hindawi
Advances in Meteorology
Volume 2023, Article ID 2346975, 18 pages
https://doi.org/10.1155/2023/2346975

Research Article

Climatology Definition of the Myanmar Southwest Monsoon (MSwM): Change Point Index (CPI)

Kyaw Than Oo [1,2]

[1]*Nanjing University of Information Science and Technology, Nanjing, China*
[2]*Aviation Weather Services, Yangon, Myanmar*

Correspondence should be addressed to Kyaw Than Oo; kyawthanoo34@outlook.com

Received 29 September 2022; Revised 30 December 2022; Accepted 9 January 2023; Published 25 January 2023

Academic Editor: Stefano Federico

Myanmar's climate is heavily influenced by its geographic location and relief. Located between the Indian summer monsoon (ISM) and the East Asian summer monsoon (EASM), Myanmar's climate is distinguished by the alternation of seasons known as the monsoon. The north-south direction of peaks and valleys creates a pattern of alternate zones of heavy and scanty precipitation during both the northeast and southwest monsoons. The majority of the rainfall has come from Myanmar's southwest monsoon (MSwM), which is Myanmar's rainy season (summer in global terms, June–September). This study explained both threshold-based and nonthreshold-based objective definitions of the onset and withdrawal of large-scale MSwM. The seasonal transitions in MSwM circulation and precipitation are convincingly represented by the new index, which is based on change point detection of the atmospheric moisture flow converging in the MSwM region (10–28 N, 92–102 E). A transition in vertically integrated moisture transport (VIMT), the reversal of surface winds, and an increase in precipitation may also be considered when defining MSwM onset objectively. We also define a change point of the MSwM (CPI) index for MSwM onset and withdrawal dates. The climatological mean onset of MSwM is day 135 (May 14), withdrawal is day 278 (October 4), and the total season length is 144 days. We are investigating spatial patterns of rainfall progression at and after the start of the monsoon, rather than transitions within a single region of the MSwM. The local southwest monsoon duration is well correlated with the CPI duration on interannual timescales, particularly in the peak rainfall regions, with a delay (advance) in large-scale onset or withdrawal associated with a delay (advance) of onset or withdrawal by local index. Hence, the next phase of this research is to study the maintenance and break of the monsoon to understand the underlying physical processes governing the monsoon circulation. The results of this study provide a possibility to reconstruct Myanmar's monsoon climate dynamics, and the findings of this study can help unravel many remaining questions regarding the greater Asian monsoon system's variability.

1. Introduction

The southwest monsoon, which sweeps across India and Southeast Asia, is among the most spectacular weather systems on the planet. Myanmar's monsoon is the most important feature for its climate variation because it is located between latitudes 09°32′N and 28°31′N and longitudes 92°10′E and 101°11′E along the Indian summer monsoon (ISM) and a large transitional zone of the Indo-China Peninsula.According to Wang and Ho (2002), [1], there are three major kinds of monsoons (Indian Monsoon (ISM), East Asian Monsoon (EASM), and Western North Pacific Summer Monsoon (WNPSM)) [2], which have already been learned (Figure 1). However, it has been discovered that Myanmar, our research area, is located in a transitional zone between two monsoon systems [2]. Also, it has been mentioned that the Indochina Peninsula is a unique place that is located between South Asia and East Asia, with the monsoon system over it displaying a transitional aspect between the South Asian and East Asian monsoons (Figure 2). Thus, it is very interesting to find the new definition and new index for this area.

Myanmar's climate is heavily influenced by its geographic location and relief, despite its location in Asia's monsoon zone. Myanmar has three seasons: summer, which

is hot and dry (March to May), southwest monsoon, which is hot and wet (June to September), and northeast monsoon, which is cold and dry (October to February) [3]. The key mechanisms of its seasons are only the northeast and southwest monsoon circulations (or winds). Central Asian cold air masses bring cold air with snow to the very northern highlands for two months annually, but the highland's mountain range prevents cold air from traveling further south of Myanmar, which is predominantly influenced by monsoon winds. Peaks and valleys that are oriented north to south create a pattern of alternate zones of heavy and scarce precipitation during both the northeast and southwest monsoons. The majority of the rainfall, on the other hand, is due to the southwest monsoon.

MSwM is the Myanmar rainy season (summer in global terms) that lasts from June to September. MSwM is also a part of the main rainy season of the Indian subcontinent. During the MSwM, the country receives nearly 75% of its annual rainfall [4]. By the middle of May, the southwest summer monsoon had settled over the peninsula's extreme southwestern point, Victoria Cliff. A rush of rainfall activity heralds the start of the monsoon. It moves in stages, finally covering the entire country by the middle of June. It began retrieving from the far northwest in early September and is now gently migrating southward.

The monsoon onset date is defined as the first day of three consecutive rainy days with a daily rainfall amount of 2.54 mm or more over Myanmar. However, the first day of three consecutive days with less than 2.54 mm over Myanmar is considered a withdrawal date. This definition is used in the Department of Meteorology and Hydrology (DMH). According to the definition of Lwin [5], the climatological southwest monsoon onset dates have been defined by using the dates with the highest frequency of long-term onsets for four different regions of Myanmar: the summer monsoon advances on May 5th in the southern Myanmar area (10°N and 15°N), over the deltaic area (15°N and 20°N) on May 15th, and on May 20th over the eastern, central, and western coasts of eastern Bay of Bengal. Another study modified with pentad (5-day averaged rainfall) analysis defined the monsoon onset dates over southern and central Myanmar on May 18 (the middle date of P28), and over northern Myanmar on May 28 (the middle date of P30) [6]. The weakness of these definitions is that they use the daily rainfall quantity of each station and thus need to omit any rainfall before April 25th as the reason that it is not the monsoon rain. Few parts of Myanmar can get rain from thunderstorm formations due to western Pacific tropical cyclones and western disturbances in winter. However, rainy days are also longer than 3 days, though the rainfall duration is very short, and wind circulation or moisture transport patterns are also important for the monsoon system. In addition to threshold-based indices being susceptible to false onsets, transient weather systems that increase rainfall in the premonsoon can also cause wind anomalies [7, 8]. For these reasons, a more objective definition of the meaningful onset and withdrawal dates of the summer southwest monsoon over Myanmar should be provided from a climatology point of view. Thus, this study's goal is to define the meaningful onset and withdrawal dates of the southwest monsoon over Myanmar objectively using long-term precipitation data, as monsoon rains are vital for agriculture and the replenishment of water resources. In this research, we provide a nonthreshold-based, objective definition of the onset and withdrawal of large-scale MSwM. The seasonal transitions in MSwM circulation and precipitation are convincingly represented by this index, which is based on change point detection of the atmospheric moisture flow converging in the large-scale MSwM sector. Vertically integrated moisture transport (VIMT) changes [9], the reversal of surface winds [10], and an increase in precipitation may also be considered when defining MSwM onset objectively.

2. Data and Methods

Data from two sets are used in the present study:

(1) Annual onset and withdrawal dates for Myanmar, daily observed rainfall data and mean sea level pressure data from 79 meteorological stations across Myanmar, were collected for validation from the Department of Meteorology and Hydrology, Myanmar (DMH).

(2) The European Centre for Medium-Range Weather Forecasts (ECMWF), ERA5 reanalysis data are used to examine the daily meteorological data (such as mean sea level pressure (MSLP), total precipitation (TP), incoming longwave radiation (OLR), and the zonal (u) and meridional (v) wind components of standard isobaric levels within the troposphere) for the years 1991–2020. It is a reanalysis dataset for global climate and weather over the last few decades with a spatial resolution of 0.25. On a global scale, ERA5 rainfall data were compared to that of the GPCP (Global Rainfall Climatology Project), which discovered that it overestimated deep convection and moisture flow convergence across tropical oceans and land, resulting in excessive rainfall [11].

The mean annual cycles of standardized rainfall and mean sea level pressure of the ERA5-gridded dataset and the data from 79 meteorological stations across Myanmar are exhibited in Figures 3(a) and 3(b). Both figures showed significant correlations between the reanalysis data and observations during 1991–2020 at a confidence level of $p < 0.05$ or 0.01 based on a two-tailed significance test, which indicates the reliability level of the reanalysis data for the next analysis.

2.1. MSWM and CPI Index. The MSwM region is defined as 10–28°N, 92–102°E (Figure 2(a), more information is available in the Tables1 and 2) which is adapted from the method of a previous study on the interannual variability of the Asia southwest monsoon, [12], and we look at seasonal shifts in the large-scale atmospheric circulation and moisture budget, as determined by the following equation:

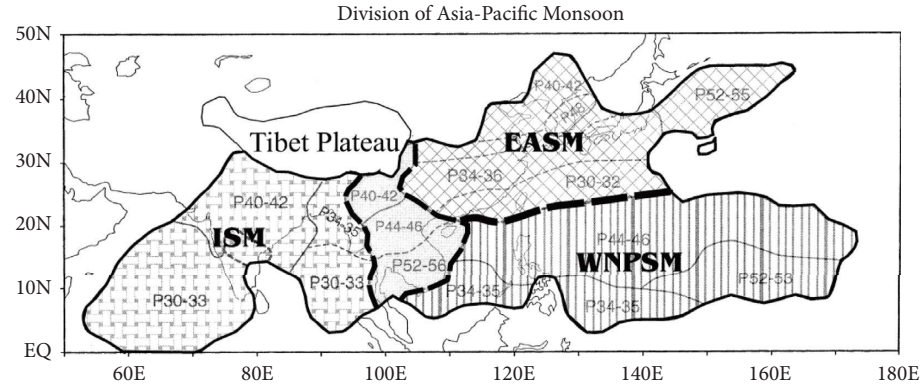

Figure 1: Map dividing the Asian-Pacific monsoon into three subregions [1].

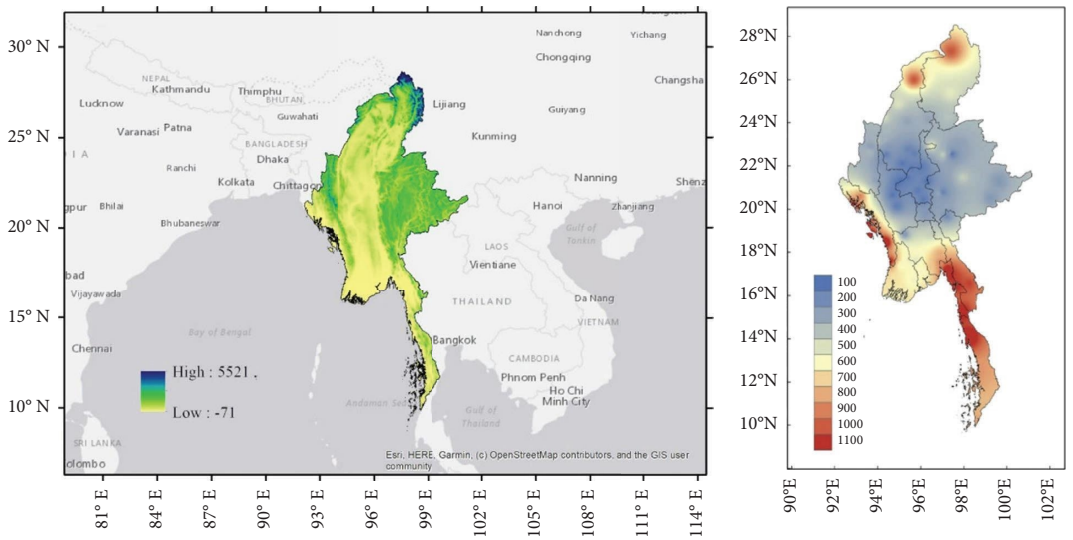

Figure 2: Study area: (a) Myanmar orography (*m*) and neighboring and (b) climatology annual total rainfall (mm) based on observation data during 1981–2020.

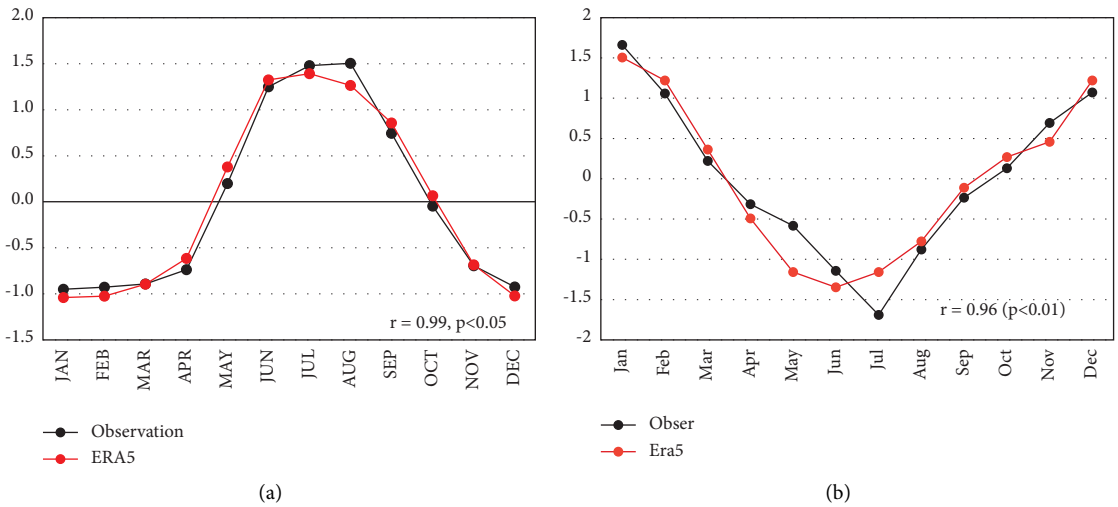

Figure 3: The mean annual cycles of standardized (a) monthly rainfall and (b) mean sea level pressure of the ERA5 and observed stations rainfall datasets, which averaged over longitudes 92°E–103°E and latitudes 10°N–30°N for the period 1991–2020.

$$\mathbf{MFC} = -\int_{\text{Surface}}^{300hPa} \nabla_p (Uq)\,\frac{dp}{g} = P - \mathrm{E} + \frac{\partial \mathrm{W}}{\partial \mathrm{t}}, \quad (1)$$

where MFC is the vertically integrated horizontal moisture flux convergence from the surface to the top of the atmosphere, "U" = (u, v) refers to the horizontal wind vector, "q" is the specific humidity, "dp" and "g" refer to the pressure differential and gravity, and all term "$\nabla_p.(Uq)$" refers to the horizontal moisture divergence/convergence in pressure levels. On the right hand, "P" is the precipitation rate and "E" is the evaporation rate, with the change of total precipitable water (W) in column "$\partial W/\partial t$" (equation (1)). There is a dominant balance between MFC and total net precipitation (P-E) with negligible storage "$\partial W/\partial t$" in the MSwM zone (e.g., Figure 4(a)). Therefore, positive MFC values and negative MFC values both refer to positive or negative net precipitation:

$$\mathbf{MSwM(CPI)} = \frac{\mathbf{1}}{\mathbf{5}} * (\mathbf{D(U1 - U2)} + \mathbf{D(P1 - P2)} + \mathbf{D(MFC)} + \mathbf{D(TPnet)} + \mathbf{D(OLR)}). \quad (2)$$

We also define a change point of the MSwM (CPI) index for MSwM onset and withdrawal, as follows: We compute the ERA5 climatology daily mean of MFC, OLR, total precipitation, and evaporation averaged over the MSwM region by each year, during 1991–2020. We also compute the climatology daily gradient of MSLP and the meridional shear of the 850 hPa zonal wind, that is, the 850 hPa zonal winds averaged over the southern Kaw Thaung region (90°E–100°E, 10°N–15°N) ($U1$, $P1$) and the northern Putao region (95°E–100°E, 25°N–30°N) ($U2$, $P2$) which is adapted from Wang et al. [13] monsoon circulation index (Figure 5).

Then, for statistical analysis, we create a standardized value for each parameter every year. The CPI onset days roughly correlate to the change from positive to negative values of daily and pentad CPI values and the revised change from negative to positive can be found in the withdrawal phase, which is a stable feature across years. In equation (2), "D" refers to the date of the change from positive to negative (negative to positive). We calculate the mean change date of the standardized positive/negative value of the pressure difference ($P1 - P2$) (dP), the meridional shear wind ($U1$-$U2$) (U-wind), the vertically integrated moisture budget transition (MFC), the net precipitation (TpNet), and the outgoing longwave radiation (OLR). In order to determine the change date, the first day of three consecutive positive or negative days is considered. Then, we got the change point dates of each variable for each year. Finally, we obtained the climatology values for all term dates (Table 3). From these results, we calculated the arithmetic mean onset dates, withdrawal dates, and season length as the MSwM Change Point Index (Table 4). The correlation coefficients of these results are determined by a student's t-test, using the 95% level of significance to ascertain t6he statistical significance of the correlation (Table 1).

Various meteorological indices, such as wind direction and speed [14], MFC [12], precipitation amount [1, 15], and OLR [16], have been employed in the previous research to determine the onset of the summer southwest monsoon. Although there is no ideal method of determining which meteorological metric best defines Myanmar's southwest summer monsoon beginning, rainfall is an operationally essential meteorological characteristic that illustrates the variability of the entire monsoon circulation system.

Thus, the CPI (Change Point Index) is constructed, which is not subject to false onsets or withdrawals because change points are using many atmospheric variables, including MFC, on all days within the defined range rather than just a single or few days' readings to examine the CPI's representativeness and explore transitions in circulation and precipitation during MSwM onset and withdrawal. We computed daily climatological composites of each atmospheric variable of the onset and withdrawal dates in each year, by using the standardized positive/negative change point method. A centered 5-day (pentad) moving average is used to smooth these composites.

The CPI index has several advantages when figuring out seasonal monsoon movements. This technique is not hampered by the drawbacks of threshold-based indices because no thresholds are utilized [17]. Finally, more than a daily average of the onset or withdrawal transition, pentad averaged change points reflected the start of the transition; the definition can be used well to more precisely characterize the transition's duration and construct composites elucidating the various timescales of the monsoon's various stages, as discussed in the following section. On interannual timescales, southwest monsoon duration is strongly correlated with CPI duration, particularly in areas experiencing peak rainfall. In large-scale onset or withdrawal, delays (advances) are associated with delays (advances) of similar magnitude in local onset or withdrawal. The climatology south west monsoon season length time series of MSwM CPI index and local

Table 1: Correlation values of parameters used in the CPI index.

	dP	*U*-wind	MFC	OLR
TP net	0.81 ($P < 0.01$)	0.8.2 ($P < 0.01$)	0.8.0 ($P < 0.01$)	−0.80 ($P < 0.01$)

Table 2: Composite of year-wise onset and withdrawal dates, season length of southwest monsoon over Myanmar as determined by the MSwM index and the DMH index, Myanmar.

Years	Onset		Withdrawal		Season length	
	MSwM	DMH	MSwM	DMH	MSwM	DMH
1991	151	146	272	270	122	125
1992	135	137	265	275	130	139
1993	134	140	275	285	142	146
1994	144	133	279	276	136	144
1995	132	135	273	276	142	142
1996	127	144	260	276	134	133
1997	132	143	278	251	148	109
1998	137	141	274	268	139	128
1999	138	130	282	273	145	144
2000	130	134	276	265	147	132
2001	122	140	265	275	144	136
2002	129	147	271	273	143	127
2003	131	137	277	268	147	132
2004	129	133	273	266	144	134
2005	145	143	276	249	132	107
2006	134	137	283	274	150	138
2007	125	134	286	282	162	149
2008	128	132	277	275	150	144
2009	138	137	286	281	149	145
2010	138	139	278	272	141	134
2011	140	142	280	283	141	142
2012	130	139	280	285	151	147
2013	136	137	275	286	141	150
2014	131	138	274	287	144	150
2015	134	137	285	286	152	150
2016	137	141	291	287	155	147
2017	150	136	299	286	150	151
2018	141	145	283	278	143	134
2019	137	144	273	270	137	127
2020	142	140	297	292	156	153

index determined by national weather service, DMH are well similar pattern during 1991–2020 (Figure 6).

3. Results and Discussion

Figure 4(a) shows an example of the climatology moisture budget circulation terms from equations (1) and (2), the MSwM time-series, and the CPI onset and withdrawal, during 1991–2020. The first blast of monsoonal rainfall is captured at the start, followed by active-break rainfall cycles throughout the monsoon season. The CPI onset (withdrawal) day corresponds approximately to the minimum (maximum) of the MSwM time series, and the transition of negative to positive (positive to negative) values of the daily pressure differential, wind differential, net precipitation, MFC, and OLR are a constant throughout all years. As a result, the term onset refers to the change from a negative precipitation budget to a positive one (and vice versa for a withdrawal budget). The onset or withdrawal dates and season lengths are measured in terms of days, from onset to withdrawal, and summarized in Figure 4(b). During the study years, the climatological onset of MSwM is day 135 (May 14th), the withdrawal is day 278 (October 4th), and the total season length is 144 days. Moreover, their standard deviations are 5, 13, and 14 days, respectively.

Using 5-day running mean (Pentad) rainfall data, Zhang [2] created the index for domain-averaged rainfall of the Southeast Asia region to determine the arrival of the southwest monsoon across the Indochina Peninsula. When compared to other Southeast Asian countries, Myanmar not only falls entirely within the Indian Monsoon (ISM) region but also the East Asian Monsoon (EASM). According to the theoretical monsoon climatic zones of Wang and Ho [1], western Myanmar exists in the ISM region, above 90°E to

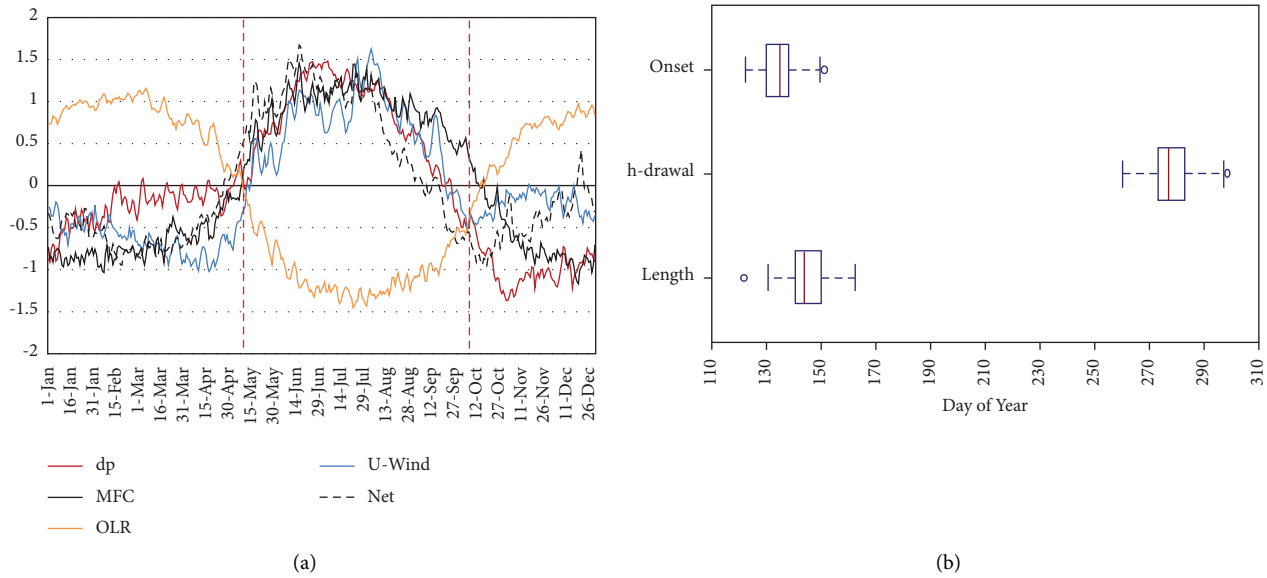

Figure 4: (a) Climatology time series of ERA-5 daily atmospheric mean sea level pressure differential averaged of northern (Putao region and southern parts (Kaw Thaung region, 25–30°N, 95–100°E) (solid red) over 10–15°N, 90–100°E during (Jan 1st, 1991–Dec 31st, 2020), the mean *U*-850 wind differential averaged as abovementioned regions (solid blue), MFC (solid black), net precipitation amount (dotted black), and CMFC (red) averaged over 10–28°N, 92–102°E. Vertical dashed red lines indicate the onset and withdrawal days in the year. (b) The seasonal onset, withdrawal, and season lengths are plotted using the MSwM box-and-whisker method. With a red median line and whiskers indicating the total range, the blue boxes show the range between the 25th and 75th percentiles.

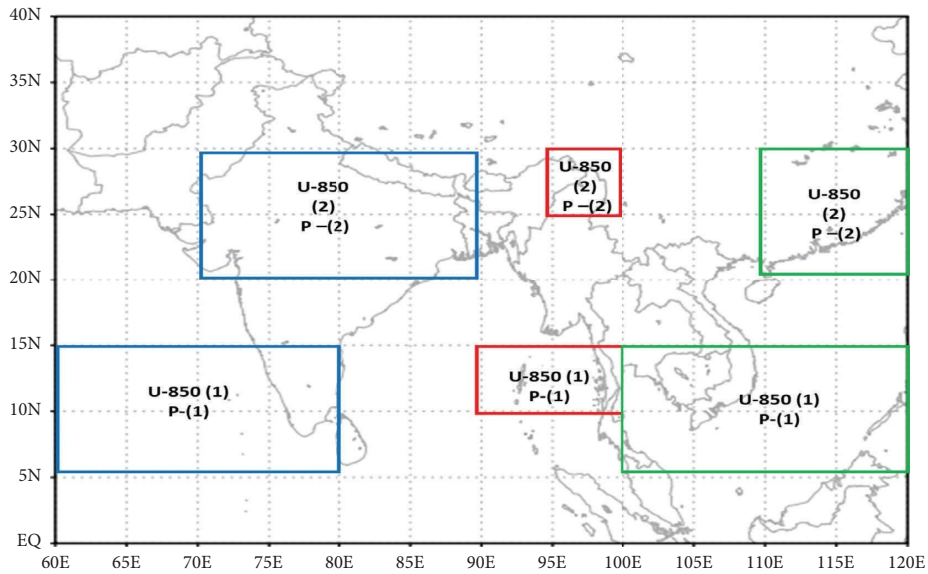

Figure 5: Typical monsoon circulation indices schematic diagrams: the ISM index (blue solid boxes), the MSwM CP index (red solid boxes), and the WNPM index (green solid boxes) were adopted from [13].

100°E, and the other part of Myanmar, which locates within the transition region of EASM is known as the northern and eastern Myanmar. Hence, the domain-averaged (92°E–102°E, 10°N–28°N) rainfall and the annual mean pentad CPI (pentad = annual precipitation/73) over Myanmar (as mentioned above) are calculated using mean pentad data from the gridded reanalysis data from 1991 to 2020. Afterward, the climatological southwest summer monsoon onset dates of Myanmar have been redefined again by using the following definition established by Matsumoto [15] for the Indochina Peninsula: "After lowering it by more than three pentads in a row, the mean pentad precipitation exceeds the yearly mean pentad precipitation in at least three pentads in a row." The start date is the middle date of this designated pentad."

Figure 7(a) displays the pentad climatology of the rainfall (mm) over Myanmar from 1991 to 2020. From mid-May until early October, the wet season in southern Myanmar is

Table 3: Comparison of monsoon onset and withdrawal dates (by day of the year) by CPI index of each parameter.

	dP	U-wind	MFC	TpNet	OLR	Mean	DMH (Mean)
Onset	135	139	136	132	135	135 (14th May)	139 (17th May)
Withdrawal	273	271	289	267	291	278 (4th Oct)	276 (1st Oct)
Length	139	133	154	136	158	144	138

Table 4: CPI index results of large-scale MSwM onset, withdrawal, and season length.

	Mean	Standard deviation	Maximum	Minimum
Onset date	135 (14th May)	5	153 (1st Jun)	120 (29th Apr)
Withdrawal date	278 (4th Oct)	13	306 (1st Nov)	255 (11th Sep)
Season length	144	14	168	117

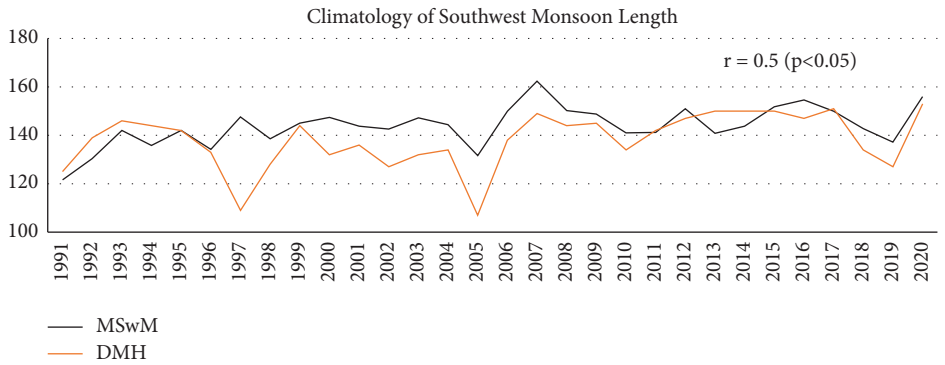

Figure 6: Climatology of MSwM and local DMH seasonal length of southwest monsoon with correlation value ($r = 0.5$) at 95% confidence level ($p < 0.05$).

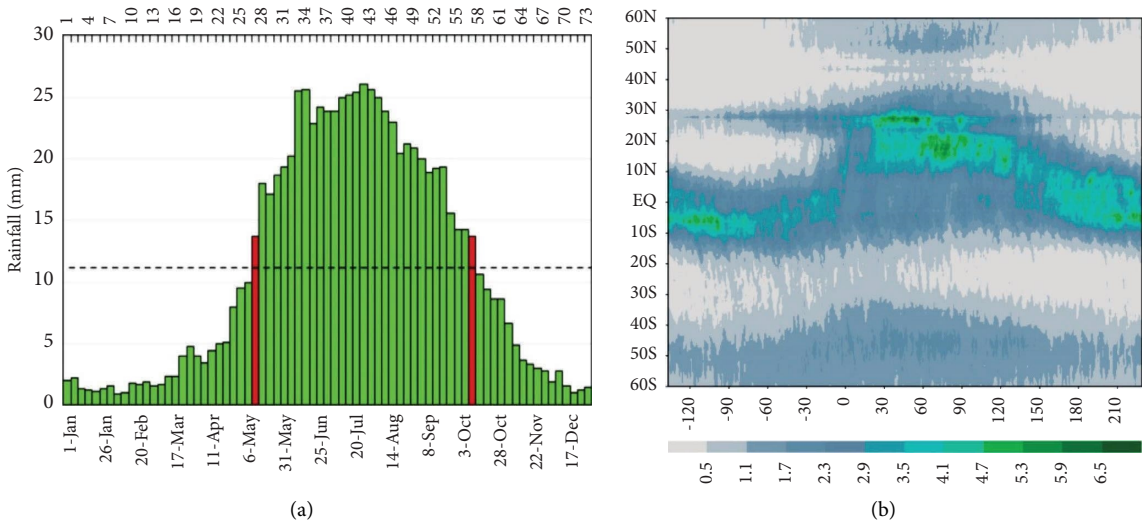

Figure 7: (a) The climatological pentad precipitation of southwest monsoon over Myanmar based on ERA5 data. The horizontal dashed line denotes the annual mean pentad precipitation (Pm) defined in the text. (b) Seasonal evolution (day of the year) of precipitation (mm·day^{-1}) averaged over 90–105°E: based on GCPC data during (Jan 1st, 1991–Dec 31st, 2020).

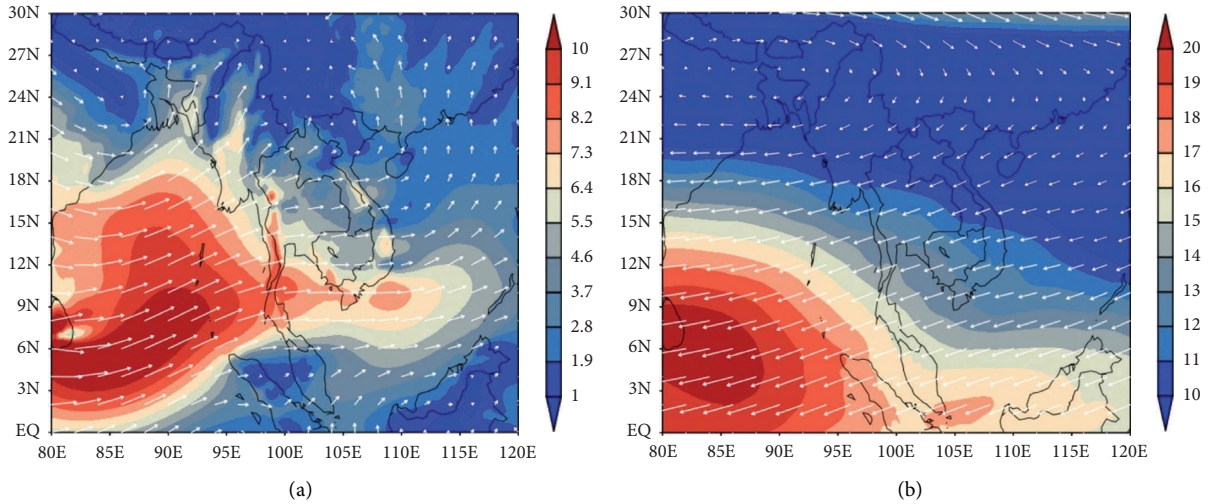

Figure 8: Climatology of southwest monsoon seasonal (JJAS) average wind speed (shaded) and direction (arrow) of (a) 850 hPa level and (b) 200 hPa level during (1991–2020).

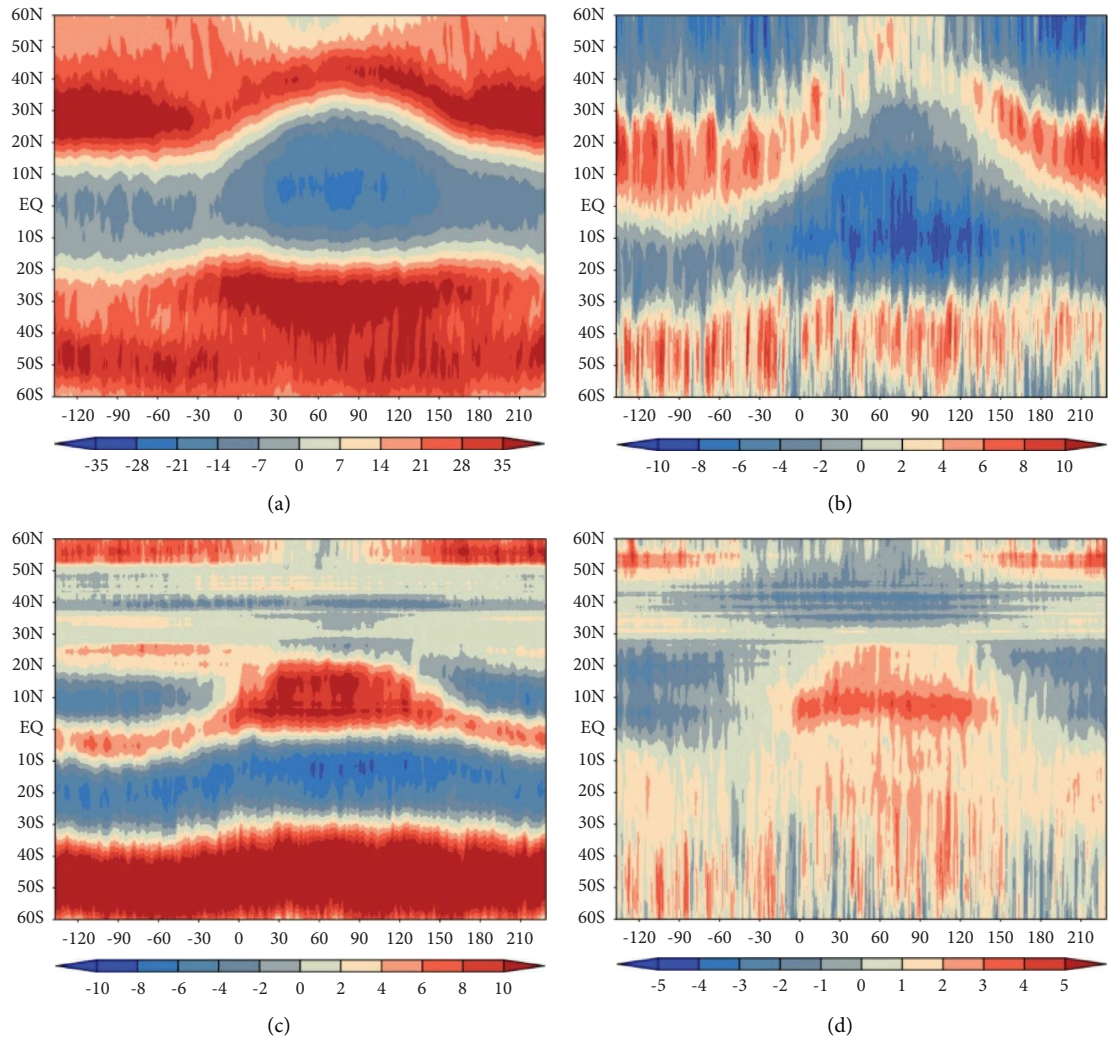

Figure 9: Climatological (1991–2020) composites centered on onset date, averaged over 90–105°E: (a) 200 hPa zonal (U_{200}) wind ($m{\cdot}s^{-1}$), (b) 200 hPa meridional (V_{200}) wind ($m{\cdot}s^{-1}$), (c) 850 hPa zonal (U_{850}) wind ($m{\cdot}s^{-1}$), and (d) 850 hPa meridional (V_{850}) wind ($m{\cdot}s^{-1}$).

well acknowledged. A rise in pentad rainfall signals the beginning of a rainy season that is greater than the yearly mean pentad precipitation (11 mm·day^{-1}). Based on the abovementioned definitions, the climatological onset date of MSwM is defined as May 14th (mean date of pentad-27), and the climatological withdrawal dates are described as October 8th (mean date of pentad-57). Figure 7(b) depicts the climatological seasonal evolution of GPCP precipitation, focused on the onset date. During the premonsoon stage, the MSwM sector (92°E–102°E) of the intertropical convergence zone (ITCZ) migrates across the equator from around 10°S to nearly 30°N, as shown by the latitude of maximum precipitation (Figure 7(b)).

The seasonal circulation of 850 hPa and 200 hPa layer wind components over the study area was found to be predominantly a large-scale overturning circulation from southwest to northeast (Figure 8). A comparable shift in the upper-level meridional (V_{200}) wind can be detected at 200 hPa. As previously established in the Eulerian mass stream function for the seasonal mean monsoon, the V_{200} field represents the upper-level flow of the large-scale meridional overturning circulation in the MSwM sector [12, 18]. There are two regional Hadley cells during the premonsoon period, with the northern hemisphere cell (NHC) initially being stronger. The southern hemisphere cell (SHC) strengthens as it expands into the northern hemisphere and the ITCZ migrates northward across the equator, while the NHC compresses and weakens (Figure 9(b)). The upper-level westerly jet weakens and migrates northward in tandem with the shift in precipitation in the northern hemisphere (NH), while a subtropical westerly jet develops in the southern hemisphere (SH) (Figure 9(a)).

In the onset stage, the ITCZ moves quickly northward, reaching about 15°N as the SH's Hadley cell suddenly becomes stronger and deeper into the NH, while the NH's Hadley cell almost disappears (Figure 9). This change is accompanied by a sudden augmentation and strengthening of upper-level tropical easterlies wind, which accompany the westerly jet's northward movement over the NH, and a strengthening of the SH's subtropical jet (Figure 9(a)).

This seasonal transition in precipitation and winds is consistent with previously reported observations for the South Asian monsoon [19–21]. It is crucial to remember that the seasonal transition in Hadley circulation is similar, as a weak or negligible summer cell occurs rather than the traditional equinoctial pattern of two Hadley cells alternating at the equinox during the summer season [22–24]. These parallels suggest that the MSwM projects heavily on the zonal mean Hadley cell and can be explained, at least in part, in terms of contemporary theories of zonal symmetry, and angular momentum conserving overturning circulations [25–27].

The onset of the MSwM occurs on a 15-day timescale, which is quite short in comparison to the seasonal cycle of insolation characterized by yearly and semiannual harmonics [28, 29]. A nearly two-fold increase in GPCP precipitation over the MSwM region from day 0 to day 15, from 1.5 mm·day^{-1} to 3 mm·day^{-1} (Figure 7(b)). We witness a seasonal change over time in each field for about two months before onset ("premonsoon"), followed by a sudden transition from day 0 to around day 20 ("onset"). By day 20, mature monsoon conditions have taken hold and will last for around three months ("mature" stage). The "withdrawal" stage is significantly more progressive than the "onset" stage, with monsoon rains gradually receding and zonal winds transitioning from weak westerly zonal wind to strong westerly zonal wind and from northerly meridional wind to southerly meridional wind over the study area during the first month of the southwest monsoon season, and the reverse pattern in the "onset" stage (Figure 9).

The same 30-day transitions in these GPCP, $U850$, and $V850$ time-series equate to significantly higher frequency variability than the monthly cycle of insolation with the best fit of the initial Fourier harmonics (based on residual least squares reduction). Figure 10 displays a sample moisture budget transportation time series in terms of equation (2), the annual accumulated time series of MFCs (since January 1) (CMFC), and CPI onset and withdrawal, climatology for 1991–2020. The first blast of monsoonal rainfall is captured at the start, accompanied by active-break rainfall cycles across the season. The CPI start day roughly correlates to the minimal of the CMFC time-series and the change from negative to positive daily MFC values, and vice versa for withdrawal, which is a stable pattern across all years. As a result, we define onset as a change in the budget of atmospheric moisture, which is the same as explained above.

3.1. Spatial Characteristics and the Local Onset. It is interesting to investigate the geographical patterns of rainfall progression at and after the monsoon's beginning, even if our index only depicts changes in the large-scale MSwM rather than a specific area of its domain. These are shown in through Figure 11 climatological composites, centered on the onset date (Pentad-27), of GPCP rainfall amount on various days in the monsoon season. Previous studies have shown that the rain belt propagates in a similar manner [1, 30]: "There is an initial development of monsoon rainfall around the eastern equatorial Indian Ocean and the eastern Bay of Bengal (BoB). Andaman Sea, Myanmar, Thailand, and Myanmar are then affected." By pentad 27, rains are established over the whole southern Myanmar region, followed by a gradual northward progression into the whole country over the following pentad of rainfall (Figure 11), as well as a revised pattern in withdrawal phases (Figure 12).

In order to know the changes in wind direction and speed over Myanmar, we display and analyze climatological mean pentad horizontal wind fields at 850 hPa and their pentad differences. When 850 hPa pentad horizontal wind patterns are displayed (Figures 13 and 14), the subtropical westerly wind moves from the northern Indian subcontinent to northern and central Myanmar between $P25$ and $P27$, then reverses during withdrawal. From $P27$, the strength of the southwest component of the equatorial westerly begins to increase in the northeastern Indian Ocean to the southern part of the BoB, reaching the southern part of the Myanmar coast (Figure 13). Over southern and central Myanmar, a distinct southwesterly wind increase can be observed in

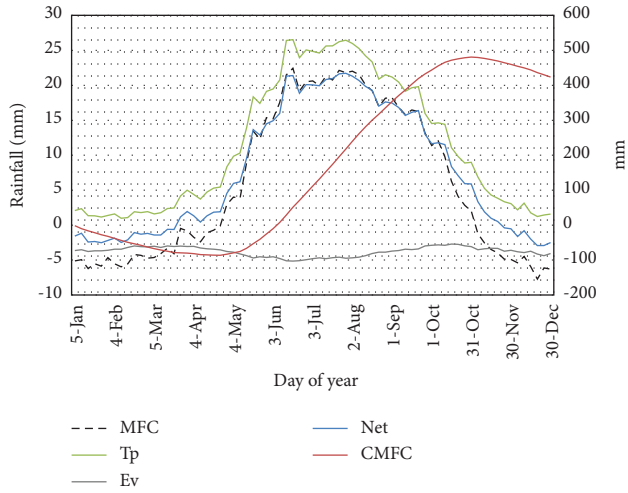

Figure 10: Climatology time-series of ERA-5 daily atmospheric moisture budget averaged over 10–30°N, 90–105°E during 1991–2020, showing the total precipitation (solid green), evaporation (solid grey), MFC (dotted black), net precipitation (solid blue), and CMFC (red).

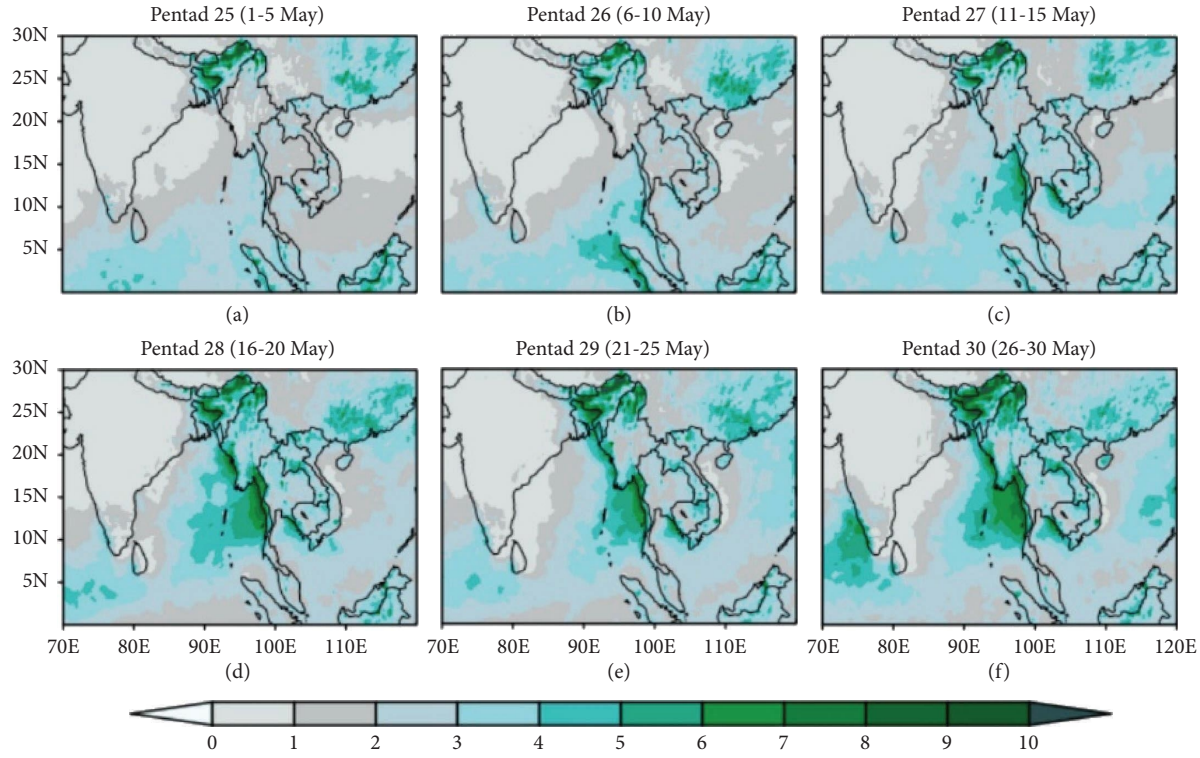

Figure 11: Composite of climatology (1991–2020) net precipitation (mm·day^{-1}, colour) during the pentads: (a) *P*-25 (May 1–5), (b) *P*-26 (May 6–10), (c) *P*-27 (May 11–15), (d) *P*-28 (May 16–20), (e) *P*-29 (May 21–25), and (f) *P*-30 (May 26–30) during monsoon onset period.

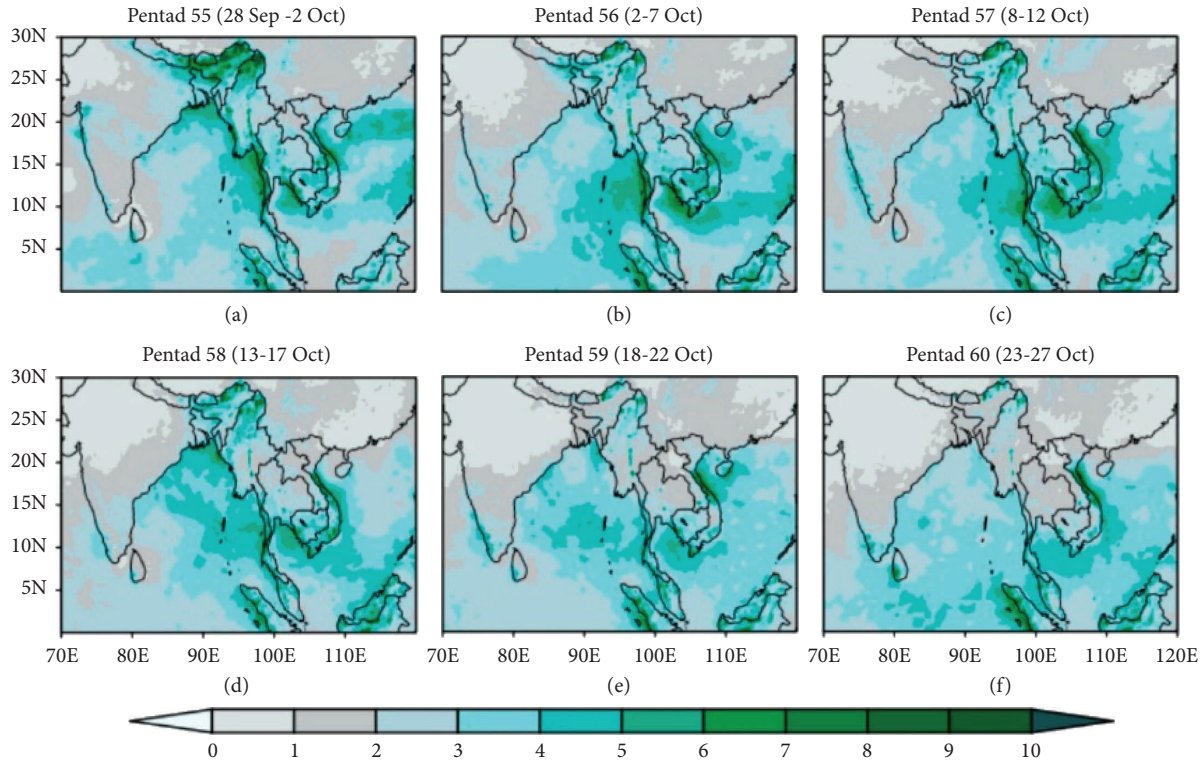

FIGURE 12: Composite of climatology (1991–2020) net precipitation (mm day^{-1}, colour) during the pentads (a) *P*-55 (Sep 28–Oct 2), (b) *P*-56 (Oct 3–7), (c) *P*-57 (Oct 8–12), (d) *P*-58 (Oct 13–17), (e) *P*-59 (Oct18–22), and (f) *P*-60 (Oct 23–27) during monsoon withdrawal period.

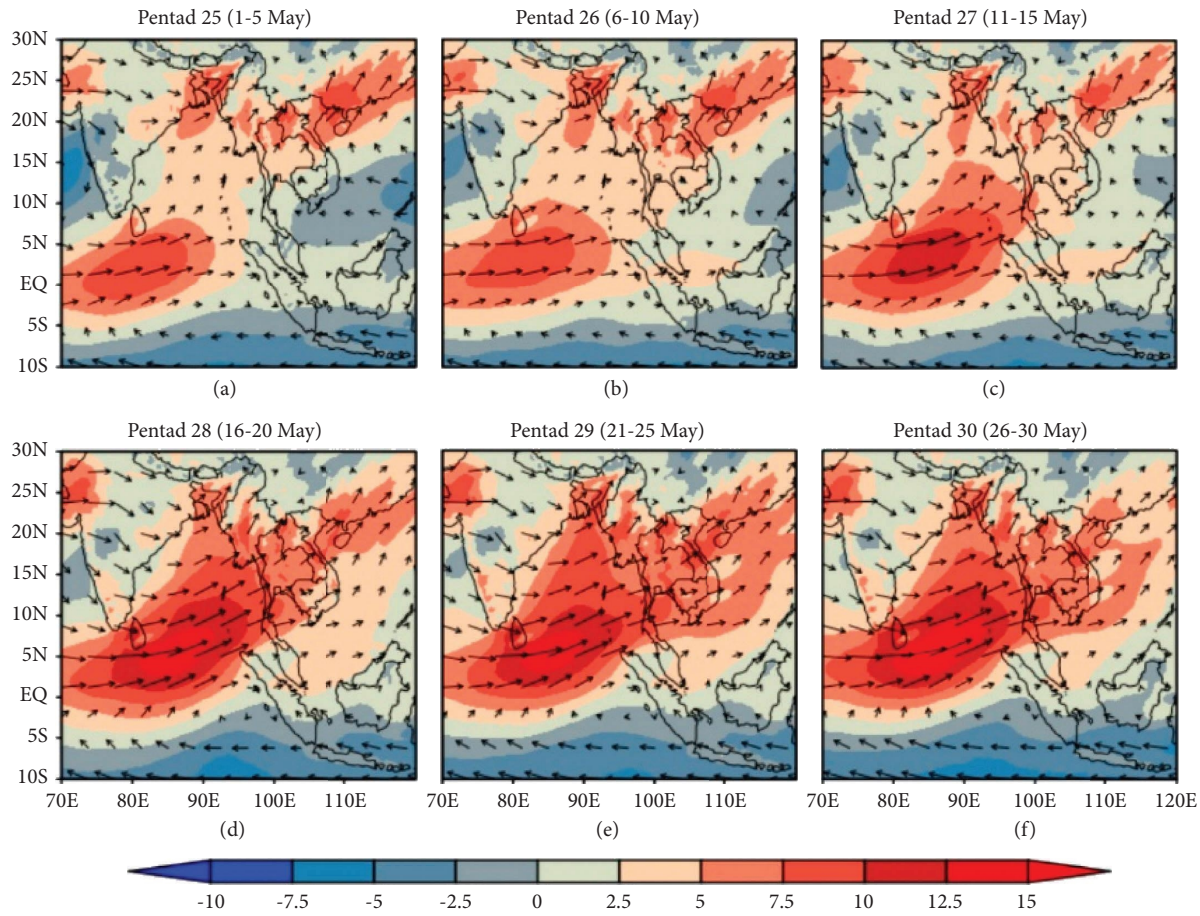

FIGURE 13: Composite of climatology (1991–2020) wind component strength (ms^{-1}, colour) and wind direction (vector arrow) at 850 hPa level during the pentads (a) *P*-25 (May 1–5), (b) *P*-26 (May 6–10), (c) *P*-27 (May 11–15), (d) *P*-28 (May 16–20), (e) *P*-29 (May 21–25), and (f) *P*-30 (May 26–30) during monsoon onset period.

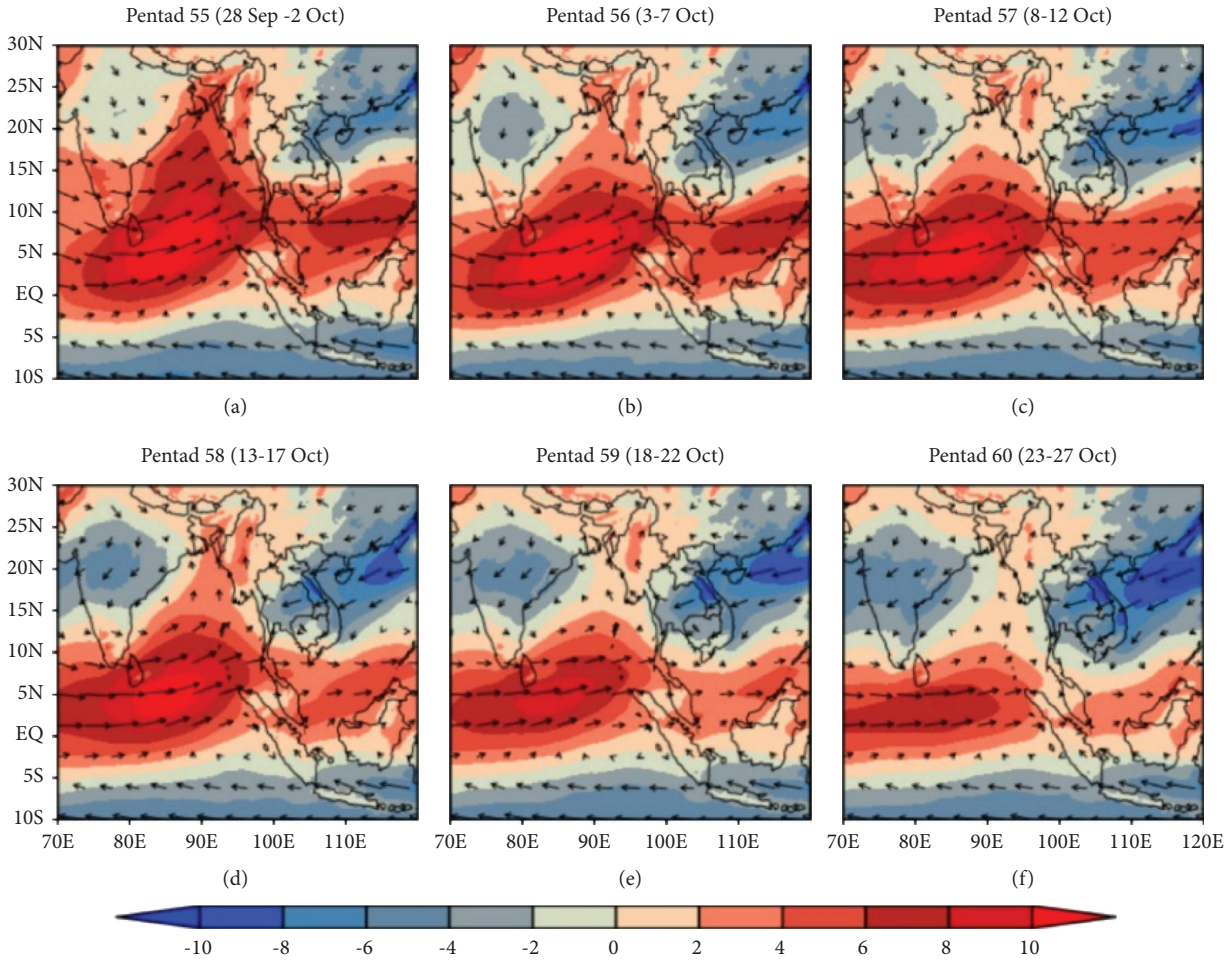

Figure 14: Composite of climatology (1991–2020) wind component strength (ms^{-1}, colour) and wind direction (vector arrow) at 850 hPa level during the pentads: (a) *P*-55 (Sep 28–Oct 2), (b) *P*-56 (Oct 3–7), (c) *P*-57 (Oct 8–12), (d) *P*-58 (Oct 13–17), (e) *P*-59 (Oct 18–22), and (f) *P*-60 (Oct 23–27) during the monsoon withdrawal period.

*P*28. However, even though the southwesterly wind dominates the entire country in *P*30, it is difficult to notice the decline in the subtropical westerly on these maps. In contrast, the reverse pattern of the abovementioned process is found during the withdrawal phases of MSwM (Figure 14). From *P*55 to *P*57, the 850 hPa wind across Myanmar did not significantly alter, however, *P*58 shows a weak westerly wind throughout central and southern Myanmar (Figure 14). Although the southwesterly wind retreats over the whole country in *P*30, the increase in subtropical easterlies cannot be clearly seen on these maps. A comparison of 6 successive pentads of 850 hPa wind was carried out in order to clarify the matter. Thus, two grid areas, the Northern Putao region (95°E–100°E, 25°N–30°N) (P_1, U_1) and Southern Kaw Thaung region (90°E–100°E, 10°N–15°N) (P_2, U_2), are selected to verify the significant period over Myanmar. In the time series of climatological pressure differential and 850 hPa zonal wind horizontal shear of two area-averaged of these grid areas, the significant change of each grid area occurs in the same *P*27 over southern and central Myanmar and *P*30 for northern Myanmar (Figures 4(a) and 9) as in other parameters in the analysis.

Figures 15 and 16 explained more details of the non-simultaneity between the dry-to-wet (wet-to-dry) transition and the wind direction reversal over the study area. The mean vertically integrated moisture of the study area was brought from the BoB, which originated from the mascarene high pressure (MHP) area over the southern Indian Ocean, before pentad 26 (equivalent to the time before May 6). Since pentad 26 (May 6–10), the MHP has gradually grown stronger and moved northward. Also, from pentad 27 (May 11 onwards), the southwest moisture flow originating from the BoB begins to prevail, marking the start of the southwest monsoon over the study area. Thus, the mean onset date fell around pentad 27.

In short, the weakening southwest monsoon gave way to winter in Myanmar. Since the 57th pentad (October 8), the Myanmar northeast monsoon (MNeM) wind has been entering from north to south, which is originating from China High Pressure (CH). Figure 16 displays the vertically integrated moisture flux of pentad 55 to 60 (i.e., September 28 to October 27). The moisture during the winter monsoon originates primarily from the northwest region, and it has become very persistent over the eastern regions of Myanmar since pentad 57

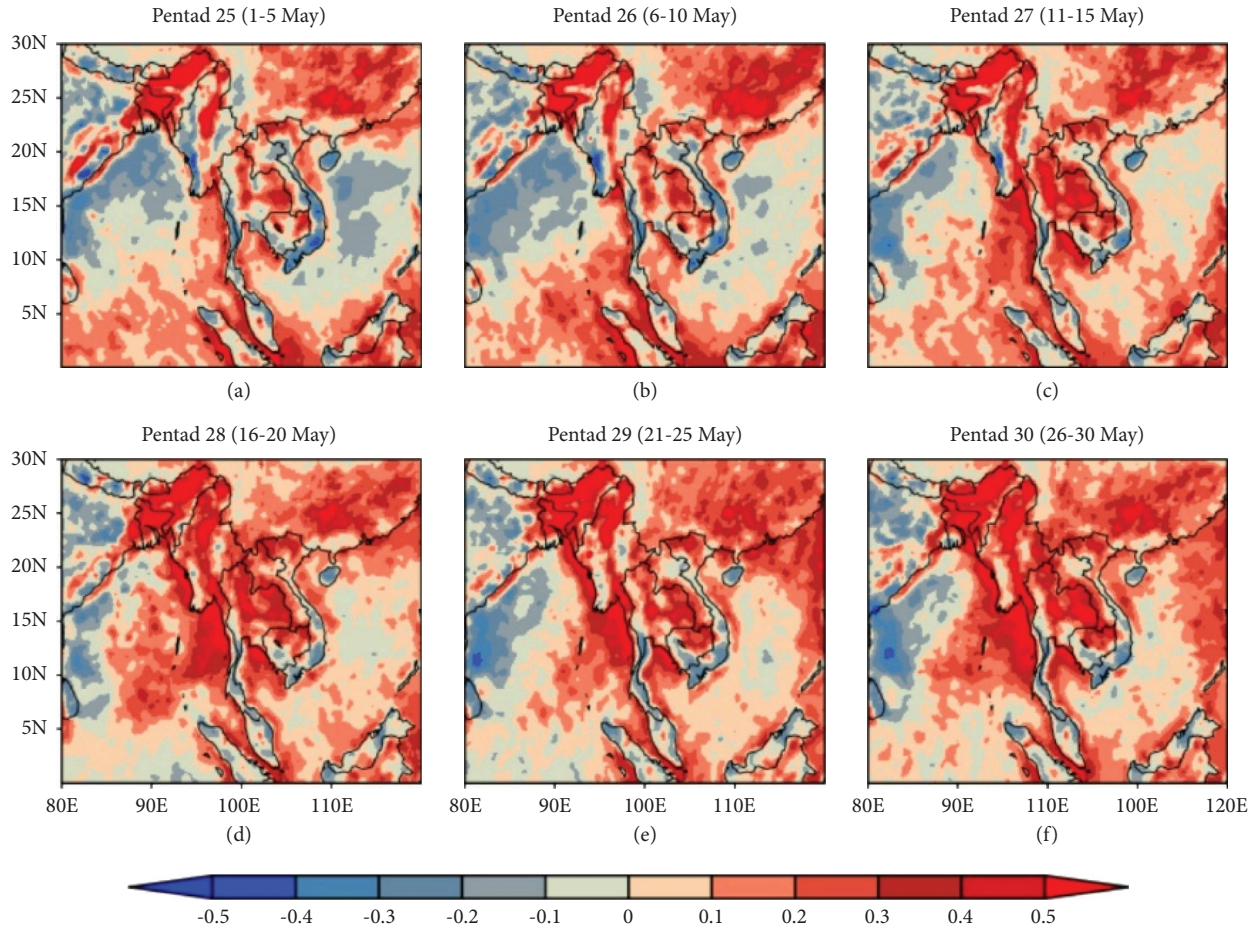

FIGURE 15: Composite of climatology (1991–2020) moisture convergence ($kg{\cdot}m^{-2}{\cdot}s^{-1}$, colour) during the pentads: (a) *P*-25 (May 1–5), (b) *P*-26 (May 6–10), (c) *P*-27 (May 11–15), (d) *P*-28 (May 16–20), (e) *P*-29 (May 21–25), and (f) *P*-30 (May 26–30) during the monsoon onset period.

(October 8). After the southwest monsoon season ends (around October-27), moisture over Myanmar is brought from the northwestern Pacific ocean by the northeast monsoon system.

Regarding the mean pentad SLP, the original 30-year mean pentad values are shown for each pentad from 1st May to 27th October without computing the distinction between two succeeding pentads of the mean pentad SLP (Figures 17 and 18). There are only two to three isobar lines with 1 hPa intervals along the eastern coast of BoB from *P*25 to *P*27 (Figures 17(a)–17(c)). But the isobar lines start to compact, and more than three isobar lines can be seen from *P*28 to *P*30 (Figures 17(d)–17(f)), which depict a rise in the southwesterly wind's velocity, which carries water vapor from BoB and the Andaman Sea to Myanmar. Time series of SLP differences two regions are drawn to assess the significant variations in SLP in order to further research this (Figure 4(a)). The withdrawal phase exhibits a significant reverse pattern (Figure 18).

The development of key parameters before MSwM onset, from two pentads before the mean onset date (*P*-25) to three pentads after the mean onset date (*P*-30), is composited for 30 years. Figure 19 presents the advancement of OLR, an equivalence to deep convection over the MSwM domain. Around May 10th (*P*-26) before onset, low OLR values (gray and blue areas) extend from the southeast BoB and Indian Ocean to the maritime continent (MC) region. Low OLR values over southeast BoB begin northwestward towards the MSwM region and extend northward along the Indochina Peninsula from May 1st (*P*-25) to May 10th (*P*-26) before MSwM onset. This is followed by a boost in convection (a new minimum value of OLR) over Southeast Asia from May 11th (*P*-27). On the biweekly time scale, the development of this new lobe is seen as a notable onset precursor [31]. Beginning on May 11th, convection strengthens two pentads in advance of MSwM, and persists until May 30th (*P*-30). The reverse pattern is also evident in the withdrawal phase (Figure 20).

A region of OLR values as low as 200 W/m^2 is shifting over the Southeast Asia region during two phases of the southwest monsoon. As MSwM approached, convective activity quickly intensified over Southeast Asia and East BoB as mentioned in [6, 32, 33]. DMH and IMD also adopt this feature as one of the parameters for objectively declaring the onset date [34, 35]. Rainfall also follows a pattern that is consistent with this OLR distribution (Figures 11 and 12) with the caveat that peak rainfall along Myanmar's coast and over the South China Sea does not always coincide with minimal OLR.

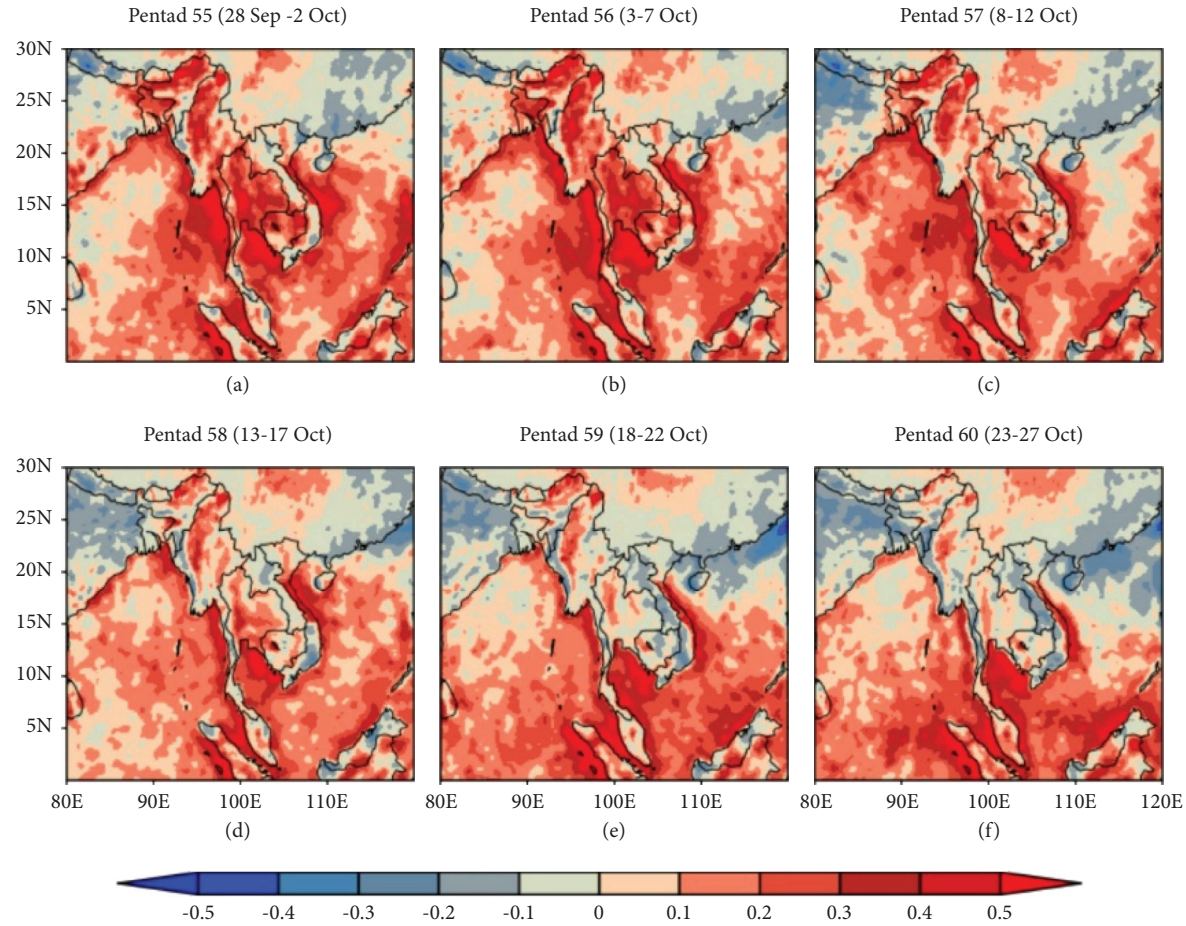

Figure 16: Composite of climatology (1991–2020) moisture convergence (kg m^{-2} s^{-1}, colour) during the pentads: (a) *P*-55 (Sep 28–Oct 2), (b) *P*-56 (Oct 3–7), (c) *P*-57 (Oct 8–12), (d) *P*-58 (Oct 13–17), (e) *P*-59 (Oct 18–22), and (f) *P*-60 (Oct 23–27) during the monsoon withdrawal period.

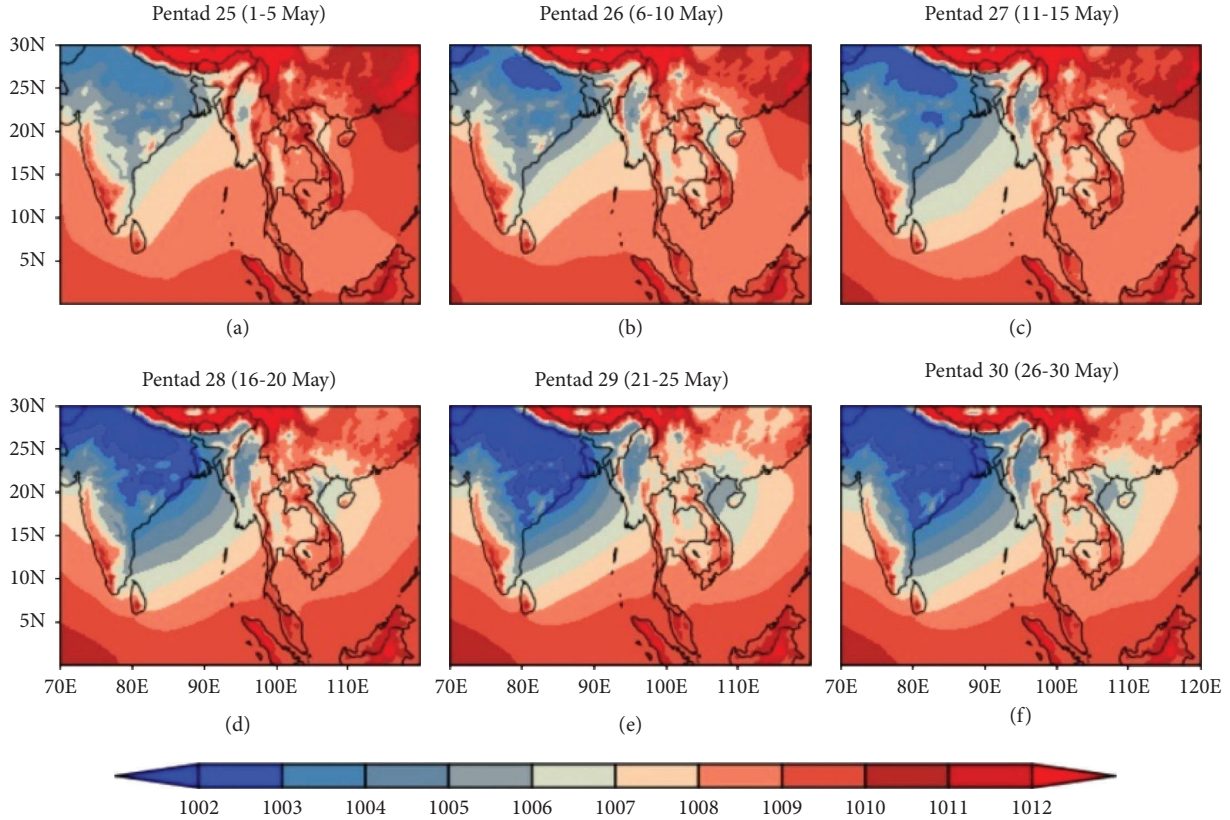

Figure 17: Composite of climatology (1991–2020) MSLP (hPa, colour) during the pentads: (a) *P*-25 (May 1–5), (b) *P*-26 (May 6–10), (c) *P*-27 (May 11–15), (d) *P*-28 (May 16–20), (e) *P*-29 (May 21–25), and (f) *P*-30 (May 26–30) during the monsoon onset period.

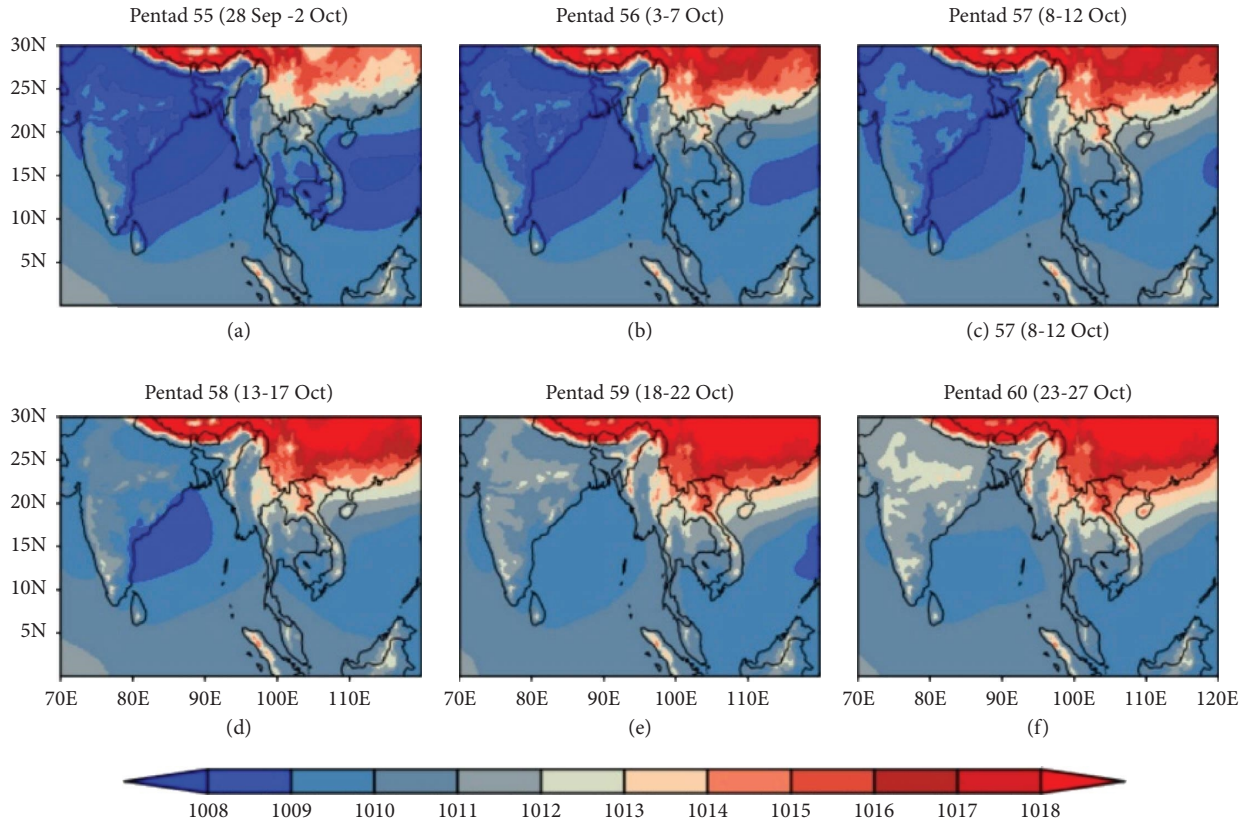

Figure 18: Composite of climatology (1991–2020) MSLP (hPa, colour) during the pentads: (a) *P*-55 (Sep 28–Oct 2), (b) *P*-56 (Oct 3–7), (c) *P*-57 (Oct 8–12), (d) *P*-58 (Oct 13–17), (e) *P*-59 (Oct 18–22), and (f) *P*-60 (Oct 23–27) during the monsoon withdrawal period.

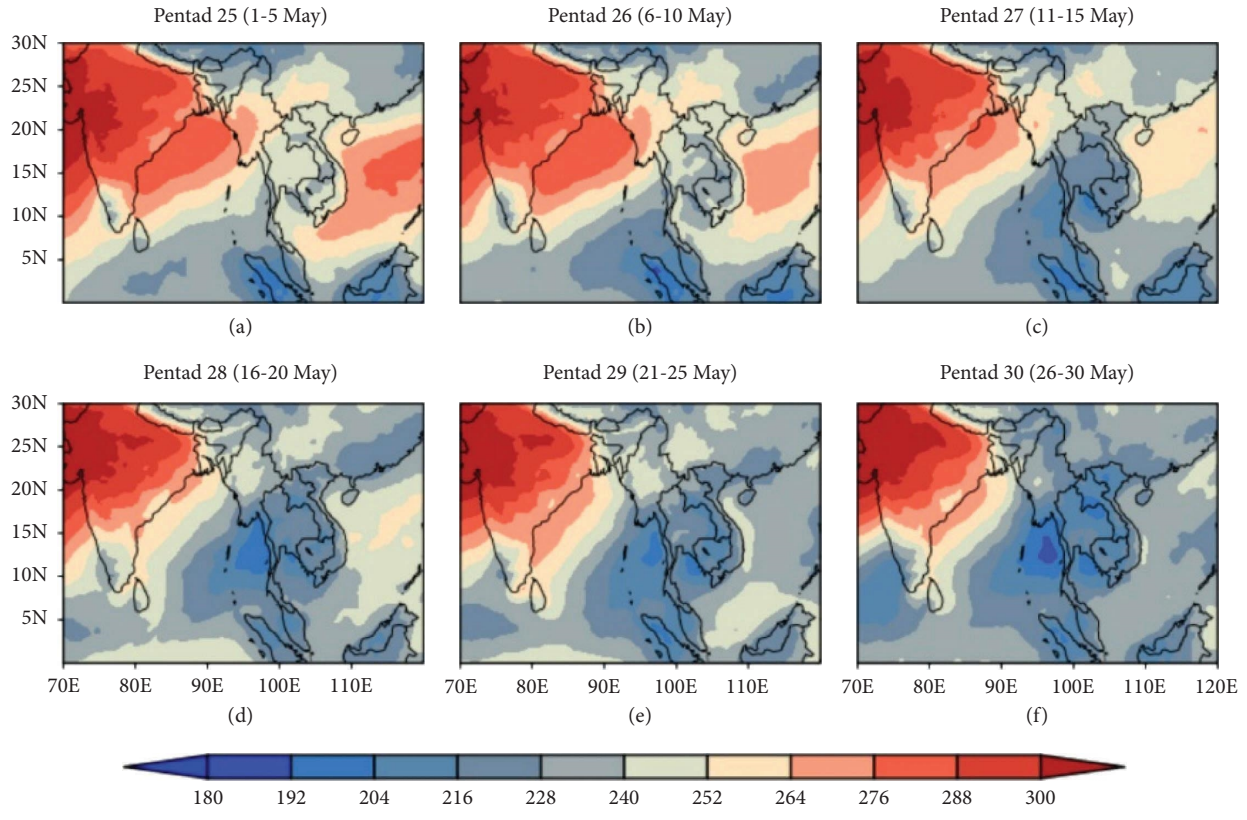

Figure 19: Composite of climatology (1991–2020) OLR (W m^{-2}, colour) during the pentads (a) *P*-25 (May 1–5), (b) *P*-26 (May 6–10), (c) *P*-27 (May 11–15), (d) *P*-28 (May 16–20), (e) *P*-29 (May 21–25), and (f) *P*-30 (May 26–30) during the monsoon onset period.

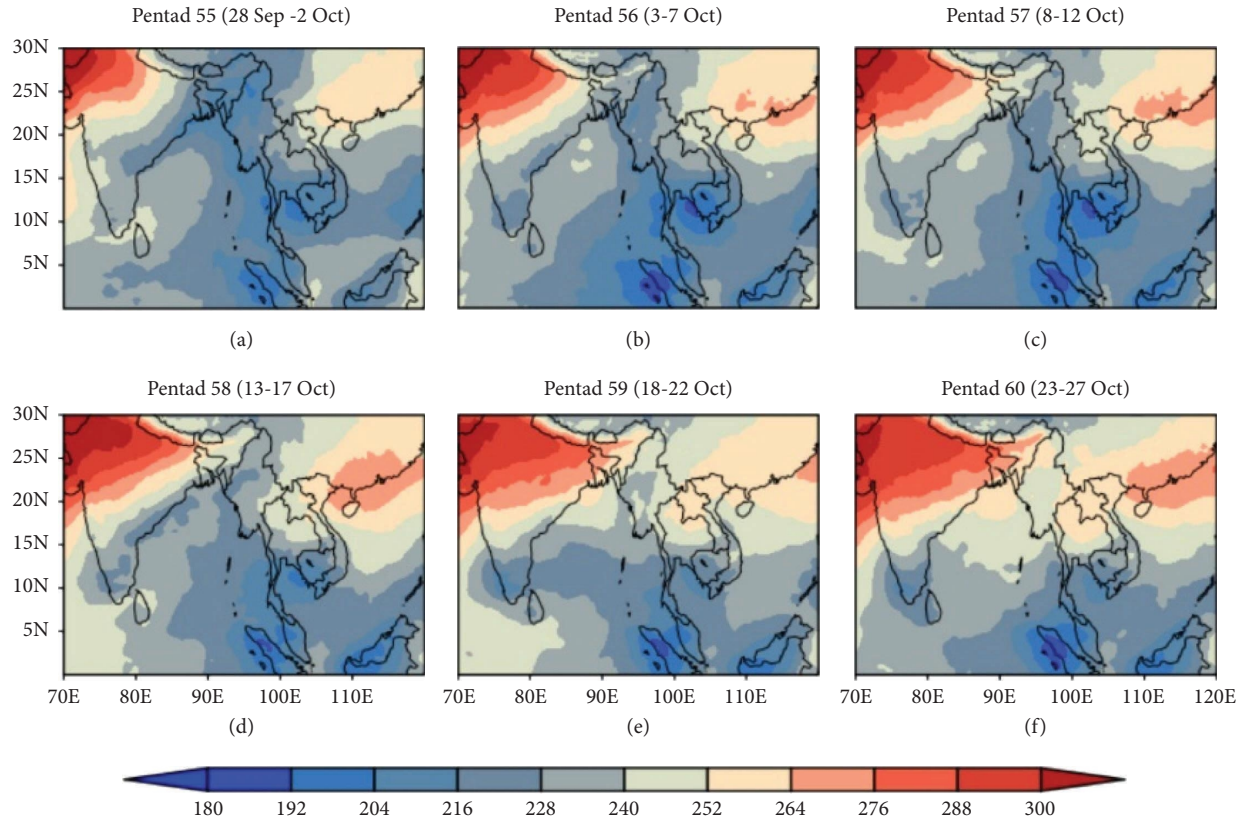

Figure 20: Composite of Climatology (1991–2020) OLR (W m^{-2}, colour) during the pentads (a) *P*-55 (Sep 28–Oct 2), (b) *P*-56 (Oct 3–7), (c) *P*-57 (Oct 8–12), (d) *P*-58 (Oct 13–17), (e) *P*-59 (Oct 18–22), and (f) *P*-60 (Oct 23–27) during the monsoon withdrawal period.

The results presented in this section demonstrate the connections between the regional changes prior to the onset and the synoptic- and even planetary-scale changes. Apparently, the latter are responsible for resulting in the former, which then leads to the onset of the summer monsoon over South China. Such causation-and-effect connections, together with some hypothesized mechanisms for these causalities, will be discussed in the next section.

4. Conclusion

The physical mechanisms that could trigger the summer southwest monsoon over Myanmar are investigated in this study. We defined the native grid of the MSwM rainfall analysis. The wording of the local definition makes it clear that it can adapt to any given spatial scale. A unique description, on the other hand, is critical for practical applications that involve understanding and forecasting the evolution of the MSwM from its earliest onset over the southern coast. We show that CPI-based dates of onset and withdrawal correspond with transitions in the monsoon circulation and the atmospheric moisture budget between negative and positive net precipitation by using data from mean pentad precipitation. The two methods are not susceptible to false onsets, making them ideal for analyzing variability, and trends in MSwM timing across datasets and climate models. The timing and abruptness of the monsoon onset are both exactly measurable by using change point detection, and we can create composites of the several monsoon stages that are distinguished by various timelines. By examining the recorded station data and reanalyzing the wind data, the date and location of the monsoon onset stage are also confirmed. Seasonal fluctuations in precipitation and circulation in the MSwM sector mean are very comparable to those in the zonal mean Hadley circulation as a result of the local ITCZ's migration and a change from the seasonal mean Hadley circulation to the MSwM sector mean. Using the CPI method to define local onset and withdrawal dates at each grid point in the MSwM domain, we find that local onset dates are approximately equal to the large-scale MSwM onset date in the southern coastal Kaw Thaung region and are progressively later further northward, with local onset dates up to one month after large-scale onset in central and northeastern Myanmar.

Regardless, testing the abovementioned hypothesis necessitates extending the search to include, if possible, the BoB, Tibetan Plateau, Indo-China, Arabian Sea, western Pacific, and south Indian Ocean. As a result of this network, we can also respond to the query of how the moderate active/weak cycle transitioned into "break" conditions. The observation in the BOB also appears to be significant from the perspective of the local experiments. The active monsoon state over Myanmar, as was previously discussed, appears to be characterized by increased convective activity across the BoB. Besides, this region is undoubtedly significant for the study of the energetics and the cyclogenesis of monsoon lows and depressions. Even with many variations in onset or

withdrawal dates, this study showed clearly how the onset of the summer monsoon over Myanmar is established. Hence, the next phase of this research is to study the maintenance and break of the monsoon to understand the underlying physical processes governing the monsoon circulation. According to our results, Myanmar's monsoon climate dynamics have significant potential for reconstruction. The findings of this study can help unravel many remaining questions regarding the greater Asian monsoon system's variability.

Data Availability

Reanalysis rainfall, component winds, OLR, and Mean Seal Level Pressure netcdf4 data for this study were downloaded from the ECMWF data portal. However, this is a fifth-generation ECMWF reanalysis dataset with a geographical resolution of 0.25 for global climate parameters over the previous decades that are used to support the findings of this study included within the article. Data are now freely available from 1950 to the present by registration at ECMWF. The actual monthly rainfall observation data from 79 observation stations used to support the findings of this study were provided under permission by Myanmar's Department of Meteorology and Hydrology (DMH) and hence cannot be freely distributed. Requests for access to these data should be made to the Director General of DMH, Myanmar (https://www.moezala.gov.mm/). Open Grads (Open-GrADS—Home), Climate data operator (https://code.mpimet.mpg.de/), and IBM SPSS are mainly used for this study. Among these first two are open source applications for everyone.

Conflicts of Interest

The author declares that there are no conflicts of interest.

Authors' Contributions

The author provided the idea, designed the study, analyzed and interpreted data, critically reviewed the article for essential intellectual content, and approved the final version of the manuscript.

Acknowledgments

The researcher expresses special thanks to all professors who approved and supported this research and Nanjing University of Information Science for supporting this research. The authors would also like to extend their gratitude to Professor Haishan Chen from Nanjing University of Information Science and Technology for supervising this paper and his other support during this research. The author acknowledges heartfelt thanks to the scientists of the ECMFW for supporting ERA5 datasets and the Department of Meteorology and Hydrology for supporting the data of Myanmar.

References

[1] B. Wang and L. Ho, "Rainy season of the asian-pacific summer monsoon," *Journal of Climate*, vol. 15, no. 4, pp. 386–398, 2002.

[2] Y. Zhang, "Onset of the summer monsoon over the indochina peninsula: climatology and interannual variations," *Journal of Climate*, vol. 15, no. 22, pp. 3206–3221, 2002.

[3] Britannica, "Myanmar - climate | britannica," 2021, https://www.britannica.com/place/Myanmar/Climate.

[4] N. Sen Roy and S. Kaur, "Climatology of monsoon rains of myanmar (Burma)," *International Journal of Climatology*, pp. 913–928, 2000.

[5] T. Lwin, "The climate changes over myanmar during the last decades," *Water Resources Journal*, 2002.

[6] O. Htway and J. Matsumoto, "Climatological onset dates of summer monsoon over myanmar," *International Journal of Climatology*, vol. 31, no. 3, pp. 382–393, 2011.

[7] M. K. Flatau, L. Talley, and P. P. Niiler, "The north atlantic oscillation, surface current velocities, and sst changes in the subpolar north atlantic," *Journal of Climate*, vol. 16, no. 14, pp. 2355–2369, 2003.

[8] R. Noska and V. Misra, "Characterizing the onset and demise of the indian summer monsoon," *Geophysical Research Letters*, vol. 43, no. 9, pp. 4547–4554, 2016.

[9] J. Fasullo and P. J. Webster, "A hydrological definition of indian monsoon onset and withdrawal," *Journal of Climate*, vol. 16, no. 19, pp. 3200–3211, 2003.

[10] C. S. Ramage, *Monsoon meteorology*, Academic Press, Cambridge, MA, USA, 1971.

[11] D. Jiao, N Xu, F Yang, and K Xu, "Evaluation of spatial-temporal variation performance of era5 precipitation data in china," *Scientific Reports*, vol. 11, no. 1, pp. 17956–13, 2021.

[12] J. M. Walker, S. Bordoni, and T. Schneider, "Interannual variability in the large-scale dynamics of the south asian summer monsoon," *Journal of Climate*, vol. 28, no. 9, pp. 3731–3750, 2015.

[13] B. Wang, R. Wu, and K. M. Lau, "Interannual variability of the asian summer monsoon: contrasts between the indian and the western north pacific-east asian monsoons," *Journal of Climate*, vol. 14, no. 20, pp. 4073–4090, 2001.

[14] J. Matsumoto, "The seasonal changes in asian and australian monsoon regions," *Journal of the Meteorological Society of Japan*, vol. 70, pp. 257–273, 1992.

[15] J. Matsumoto, "Seasonal transition of summer rainy season over indochina and adjacent monsoon region," *Advances in Atmospheric Sciences*, vol. 14, no. 2, pp. 231–245, 1997.

[16] T. Murakami and J. Matsumoto, "Summer monsoon over the asian continent and western north pacific," *Journal of the Meteorological Society of Japan*, vol. 72, no. 5, pp. 719–745, 1994.

[17] J. M. Walker, *Seasonal and Interannual Variability in South Asian Monsoon Dynamics Thesis by*, 2017.

[18] S. Bordoni and T. Schneider, "Monsoons as eddy-mediated regime transitions of the tropical overturning circulation," *Nature Geoscience*, vol. 1, no. 8, pp. 515–519, 2008.

[19] C. Li and M. Yanai, "The onset and interannual variability of the asian summer monsoon in relation to land-sea thermal contrast," *Journal of Climate*, vol. 9, no. 2, pp. 358–375, 1996.

[20] K. E. Trenberth and D. J. Shea, "Relationships between precipitation and surface temperature," *Geophysical Research Letters*, vol. 32, no. 14, pp. 1–4, 2005.
[21] P. J. Webster and S. Yang, "Monsoon and enso: selectively interactive systems," *Quarterly Journal of the Royal Meteorological Society*, vol. 118, no. 507, pp. 877–926, 1992.
[22] I. M. Dima and J. M. Wallace, "On the seasonality of the hadley cell," *Journal of the Atmospheric Sciences*, vol. 60, no. 12, pp. 1522–1527, 2003.
[23] H. Nguyen, A. Evans, C. Lucas, I. Smith, and B. Timbal, "The hadley circulation in reanalyses: climatology, variability, and change," *Journal of Climate*, vol. 26, no. 10, pp. 3357–3376, 2013.
[24] T. A. Shaw, "On the role of planetary-scale waves in the abrupt seasonal transition of the northern hemisphere general circulation," *Journal of the Atmospheric Sciences*, vol. 71, no. 5, pp. 1724–1746, 2014.
[25] S. Gadgil, "The indian monsoon and its variability," *Annual Review of Earth and Planetary Sciences*, vol. 31, no. 1, pp. 429–467, 2003.
[26] N. C. Privé and R. A. Plumb, "Monsoon dynamics with interactive forcing. part I: axisymmetric studies," *Journal of the Atmospheric Sciences*, vol. 64, no. 5, pp. 1417–1430, 2007.
[27] T. Schneider and S. Bordoni, "Eddy-mediated regime transitions in the seasonal cycle of a hadley circulation and implications for monsoon dynamics," *Journal of the Atmospheric Sciences*, vol. 65, no. 3, pp. 915–934, 2008.
[28] W. R. Boos and K. A. Emanuel, "Annual intensification of the somali jet in a quasi-equilibrium framework: observational composites," *Quarterly Journal of the Royal Meteorological Society*, vol. 135, no. 639, pp. 319–335, 2009.
[29] K. M. Weickmann and R. M. Chervin, "The observed and simulated atmospheric seasonal cycle. part I: global wind field modes," *Journal of Climate*, vol. 1, no. 3, pp. 265–289, 1988.
[30] Y. Wang, S. Li, and D. Luo, "Seasonal response of asian monsoonal climate to the atlantic multidecadal oscillation," *Journal of Geophysical Research*, vol. 114, no. D2, Article ID D02112, 2009.
[31] B. Wang, Q. Ding, and P. V. Joseph, "Objective definition of the indian summer monsoon onset," *Journal of Climate*, vol. 22, no. 12, pp. 3303–3316, 2009.
[32] L. L. Aung, *Myanmar Climate Report*, Norwgian Meterological Institute, no. 9, , p. 105, Oslo, Norway, 2017.
[33] Z. M. M. Sein and X. Zhi, "Interannual variability of summer monsoon rainfall over myanmar," *Arabian Journal of Geosciences*, vol. 9, no. 6, p. 469, 2016.
[34] D. S. Pai and R. M. Nair, "Summer monsoon onset over kerala: new definition and prediction," *Journal of Earth System Science*, vol. 118, no. 2, pp. 123–135, 2009.
[35] Z. M. Mie Sein, I. Ullah, F. Saleem, X. Zhi, S. Syed, and K. Azam, "Interdecadal variability in myanmar rainfall in the monsoon season (may–october) using eigen methods," *Water (Switzerland)*, vol. 13, no. 5, p. 729, 2021.